Available online at www.sciencedirect.com
SCIENCE DIRECT®
International Journal of Mass Spectrometry 230 (2003) 57–64
International Journal of Mass Spectrometry
www.elsevier.com/locate/ijms

Efficiency of energy transfer in protonated diglycine and dialanine SID Effects of collision angle, peptide ion size, and intramolecular potential

Jiangping Wang, Samy O. Meroueh, Yanfei Wang, William L. Hase*

Departments of Chemistry and Computer Science, Wayne State University, Detroit, MI 48202, USA

Received 23 April 2003; accepted 13 August 2003

Abstract

Classical trajectory simulations are performed to study energy transfer in collisions of protonated diglycine, $(gly)_2H^+$, and dialanine, $(ala)_2H^+$, ions with the diamond {1 1 1} surface, for a collision energy E_i in the range of 5–110 eV and incident angles of 0 and 45° with respect to the surface normal. The distribution of energy transfer to vibrational/rotational degrees of freedom, ΔE_{int}, and to the surface, ΔE_{surf}, and of energy remaining in peptide ion translation, E_f, are very similar for $(gly)_2H^+$ and $(ala)_2H^+$. The average percent energy transferred to ΔE_{surf} and E_f increases and decreases, respectively, with increase in E_i. Average energy transfer to ΔE_{int} is less dependent on E_i, but does decrease with increase in E_i. The AMBER and AM1 models for the $(gly)_2H^+$ intramolecular potential give statistically identical energy transfer distributions in $(gly)_2H^+$ + diamond {1 1 1} collisions. A comparison of the current study with previous trajectory simulations of $glyH^+$, $(gly)_3H^+$, and $(gly)_5H^+$ collisions with diamond {1 1 1} shows that the energy transfer efficiencies to ΔE_{int}, ΔE_{surf}, and E_f are similar for $(gly)_nH^+$, $n = 1$–5. The energy transfer distributions for $(gly)_2H^+$ + diamond {1 1 1} collisions depend on the collision angle and do not scale in accord with the normal component of the collision energy E_i^n for collisions with θ_i of 0 and 45°.

Keywords: Surface-induced dissociation; Peptide ions; Trajectory simulations; Energy transfer

1. Introduction

Surface-induced dissociation (SID) is used to study the mechanisms and energetics for ion fragmentation [1–5]. In addition, the fragmentation products provide a fingerprint of the ion's structure, and SID may become an important tool for determining the amino acid sequence of protonated peptide ions [2,6–14]. In a typical experiment [1], a beam of ions, each with a fixed translational energy E_i and incident angle θ_i, strikes a surface. Some of each ion's translational energy is transferred to surface vibration, ΔE_{surf} and to the ion's internal vibrational/rotational degrees of freedom, ΔE_{int}, while some remains in translation E_f: i.e.,

$$E_i = E_f + \Delta E_{surf} + \Delta E_{int} \quad (1)$$

This energy transfer model assumes that the collisions are electronically adiabatic and the excitation of electronic states of either the projectile or surface are important. Such a model is consistent with experiments with peptide ions and hydrocarbon surfaces, which do not have low-lying electronic states. If an excited electronic state is formed in the collision, it is assumed that it undergoes rapid internal conversion to its ground electronic state, which has a much higher vibrational density of states.

To interpret SID experiments, it is very useful to know the distributions of percent energy transfer to ΔE_{int}, ΔE_{surf}, and E_f and how they depend on E_i and θ_i, the projectile ion's size and shape, and properties of the surface. Classical trajectory simulations, based on accurate potentials for the projectile–surface system, have proven to be an important method for determining these energy transfer distributions [15–19]. For $Cr^+(CO)_6$ SID the ΔE_{int} energy transfer distribution determined from the simulations [17] is in quantitative agreement with experiment [20]. Simulations of energy transfer in protonated glycine, triglycine, and pentaglycine SID [18,19] give ΔE_{int} energy transfer distributions similar to the one determined from experiment for protonated dialanine [12]. A power of the trajectory simulations is that they may be used to determine energy transfer distributions, study specific systems, and answer important questions concerning SID dynamics that are difficult to probe experimentally.

* Corresponding author. Tel.: +1-313-577-2694; fax: +1-313-577-8822.
E-mail address: wlh@cs.wayne.edu (W.L. Hase).

1387-3806/$ – see front matter © 2003 Elsevier B.V. All rights reserved.
doi:10.1016/j.ijms.2003.08.005

In the work presented here, trajectory simulations are used to compare the energy transfer distributions for protonated diglycine, $(gly)_2H^+$, and protonated dialanine, $(ala)_2H^+$, colliding with the diamond {1 1 1} surface. This work is an extension of previous simulations of $glyH^+$, $(gly)_3H^+$, and $(gly)_5H^+$ SID [18,19] and the energy transfer distributions determined from the current $(gly)_2H^+$ study are compared with those of the previous simulations to see how the energy transfer efficiencies to ΔE_{int}, ΔE_{surf}, and E_f depend on peptide size. Both the AMBER [21] and AM1 [22] potential energy models are used to represent the intramolecular potential for $(gly)_2H^+$, to determine whether they give the same or different energy transfer efficiencies. Different incident angles θ_i are used in experiments [1–14] and, to study the effect of the incident angle on the energy transfer distributions, both θ_i of 0 and 45° with respect to the surface normal are considered in the current simulations of $(gly)_2H^+$ + diamond {1 1 1} collisions.

2. Computational method

The method used for the simulations reported here is the same as that used in previous simulations of protonated peptide ion SID [18,19]. The simulations were performed with the VENUS [23] and VENUS/MOPAC [24,25] computer program packages. Only a brief description of the simulation method is given below.

2.1. Potential energy function

The general analytic potential energy function used for the protonated peptide/diamond {1 1 1} systems is given by:

$$V = V_{peptide} + V_{surface} + V_{peptide,surface} \quad (2)$$

where $V_{peptide}$ is the protonated peptide intramolecular potential, $V_{surface}$ is the potential for the diamond surface, and $V_{peptide,surface}$ is the peptide/diamond intermolecular potential. For most of the simulations reported here the AMBER valence force field of Cornell et al. [21] was used for the $(gly)_2H^+$ and $(ala)_2H^+$ intramomolecular potentials. The minimum energy conformers of these peptide ions, shown in Fig. 1, were used in the simulations. A local energy minimization algorithm of the VENUS computer program was used to determine the conformer structures. There is a slightly higher energy conformer for $(gly)_2H^+$ and $(ala)_2H^+$ with the H atom of the OH group rotated 90°, so that the OH bond is in a plane nearly perpendicular to the plane of the peptide backbone. Unpublished simulations for $(gly)_2H^+$ [26] show that this higher energy conformer and the mini-

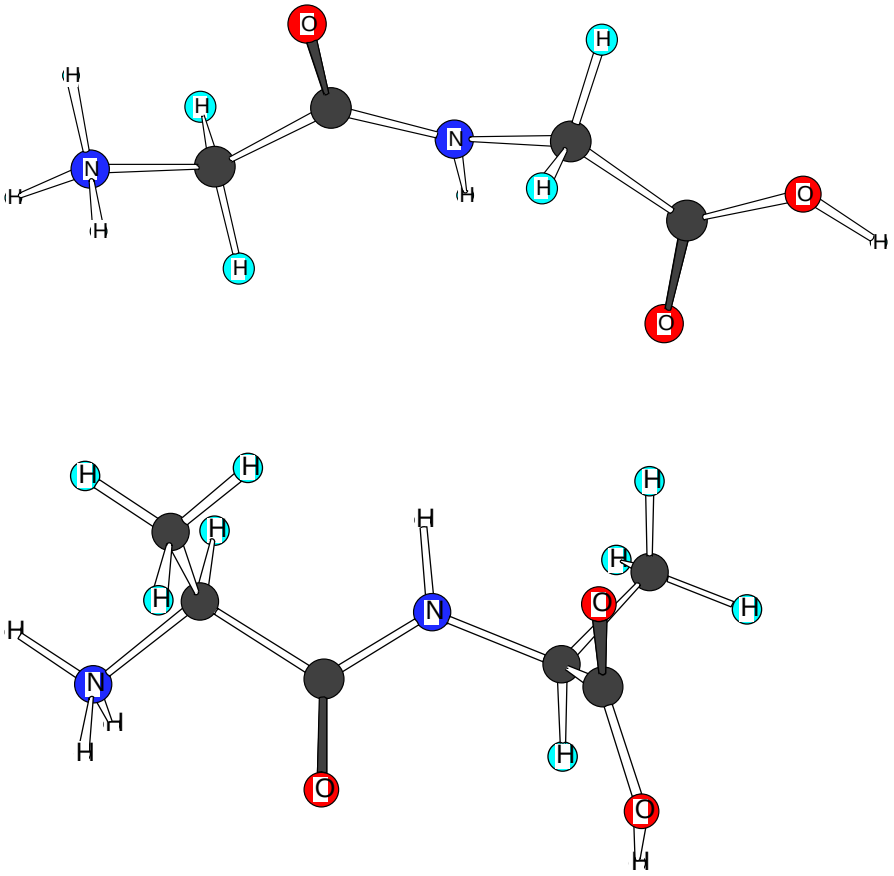

Fig. 1. Conformers of protonated diglycine and dialanine studied in the simulations. A 300 K Boltzmann distribution of vibrational energy was added to the conformer, for each ensemble of trajectories calculated.

mum energy conformer in Fig. 1 give the same energy transfer efficiencies when colliding with the diamond {1 1 1} surface. To investigate whether the energy transfer efficiencies depend on the form of the peptide ion's intramolecular potential, simulations were also performed in which the $(gly)_2H^+$ potential is modeled by AM1 semiempirical electronic structure theory [22]. The $(gly)_2H^+$ conformer in Fig. 1 was also used for these calculations with AM1.

The model used for the diamond surface is hydrogen terminated, with eight layers of carbon atoms and a total of 1988 atoms. It has a surface area of 34 Å × 34 Å and a thickness of 8.0 Å from the top hydrogen atoms to the bottom carbon atoms (see Fig. 1 in Ref. [17]). Massive atoms are attached to the bottom corner atoms of the model to ensure the model did not move when struck by peptide ions. The potential energy function for the diamond {1 1 1} model consists of harmonic stretches and bends, with force constants chosen to fit the diamond phonon spectrum [27].

Accurate repulsive potentials between the colliding peptide ion and the surface are necessary to accurately describe energy transfer in peptide SID. Such potentials were developed in previous work [18] for peptide ions interacting with hydrocarbon surfaces, such as diamond {1 1 1}. These potentials were derived from high level ab initio potential energy curves [18] for the interaction between CH_4, as a model for the C and H atoms of the hydrocarbon surface and CH_4, NH_3, CH_4^+, H_2CO, and H_2O as models for the different types of atoms and functional groups comprising the peptide. These potential curves are accurately fit by a sum of two-body potentials, each given by:

$$V_{xy}(r_{ij}) = A_{xy}\exp(-B_{xy}r_{ij}) + \frac{C_{xy}}{r_{ij}^6} \quad (4)$$

where x corresponds to C or H atoms of CH_4 and y corresponds to H, C, O, or N atoms of the model molecules representing the peptide ion's atoms and functional groups. $V_{\text{peptide,surface}}$ for $(gly)_2H^+$ and $(ala)_2H^+$ interacting with the diamond {1 1 1} surface was written as a sum of these two-body potentials.

2.2. Trajectory simulations

The classical trajectory [28,29] simulations were carried out with the general chemical dynamics package VENUS [23] for the calculations with the AMBER intramolecular potential, and with the VENUS/MOPAC [25] package for the calculations with the AM1 intramolecualr potential. Initial conditions for the trajectories were chosen to model experiments. The center of a beam of peptide ion projectiles is aimed at the center of the surface, with fixed incident angle θ_i with respect to the surface normal and fixed initial translational energy E_i. The radius of the beam was chosen so that the beam overlapped a unit area on the surface and the trajectory results are insensitive to its radius. The peptide projectile for each trajectory was randomly placed in the cross-section of this beam and randomly rotated about its center of mass so that it has an initial random orientation with respect to the surface. The azimuthal angle χ, between the beam and a fixed plane perpendicular to the surface, was sampled randomly between 0 to 2π. Such a random sampling of χ simulates collisions with different domains of growth on the diamond surface [17]. The distance between the center of the beam and the center of the top of the surface was set to 40 Å.

The initial conditions for the vibrational modes of the peptide ions were chosen via the quasiclassical normal mode method [30–33], which includes zero-point energies. Excess energies, for each normal mode of vibration, were selected from the mode's 300 K quantum harmonic oscillator Boltzmann distribution. The energy was randomly partitioned between kinetic and potential by choosing a random phase for each normal mode. A 300 K rotational energy of $RT/2$ was added to each principal axis of rotation of peptide.

To assign an initial condition representing a 300 K Boltzman distribution for the atoms of the diamond surface, the surface was first equilibrated for 1 ps of molecular dynamics by scaling the atomic velocities [34] so the surface temperature corresponds to that for 300 K classical Boltzmann distributions. The structure and velocity obtained from this equilibration process is then used as the initial structure for an equilibration run at the beginning of each trajectory. A time step of 0.1 fs was used to integrate the classical equations of motion, to ensure conservation of energy to eight significant figures.

The trajectories for $(gly)_2H^+$ and $(ala)_2H^+$ colliding with diamond {1 1 1} were calculated for a collision angle θ_i of 45° and collision energies E_i of 5, 10, 30, 70, and 110 eV. Trajectories were calculated for $(gly)_2H^+$ colliding with the diamond surface at θ_i of 0° and E_i of 30, 70, 110 eV. Three hundred trajectories were computed for each set of initial conditions with fixed E_i and θ_i. When the trajectory is terminated, the peptide ion's final translational energy, E_f, is determined and the ion's internal energy change, ΔE_{int}, is determined by subtracting the initial value of the projectile's internal energy from its final value. The energy transferred to the surface, ΔE_{surf}, is then determined from the energy conservation relationship Eq. (1).

3. Energy transfer distributions and efficiencies

3.1. Protonated diglycine and dialanine

The average percents of the collision energy E_i that remains in translation, E_f, transferred to the surface, ΔE_{surf}, or transferred to the peptide's internal degrees of freedom, ΔE_{int}, are listed in Table 1 for $(gly)_2H^+$ and $(ala)_2H^+$ collisions with diamond {1 1 1} at a collision angle θ_i of 45°. The energy transfer efficiencies are very similar for these two dipeptides. For all collision energies, the majority of E_i remains in final translational energy E_f. However, the percent remaining in translation decreases with increase in E_i

Table 1
Average percent energy transfer[a]

E_i (eV)	$(gly)_2H^+$, $\theta_i = 45°$			$(ala)_2H^+$, $\theta_i = 45°$			$(gly)_2H^+$, $\theta_i = 0°$		
	ΔE_{int}	ΔE_{surf}	E_f	ΔE_{int}	ΔE_{surf}	E_f	ΔE_{int}	ΔE_{surf}	E_f
5	16	0	84	19	1	80	–	–	–
10	17	4	79	19	5	76	–	–	–
30	16	12	72	18	12	70	24	27	49
70	15	25	60	21	21	58	20	40	40
110	13	34	53	15	31	54	17[b]	48[b]	35[b]

[a] The results given here are for calculations with the AMBER intramolecular potential for the protonated peptide. The AM1 intramolecular potential gives the same results for the $(gly)_2H^+$, $\theta_i = 0°$ calculations.
[b] E_i for this calculation is 100 eV.

and the percent energy transfer to surface. Though the percent energy transfer to the internal degrees of freedom of $(gly)_2H^+$ and $(ala)_2H^+$ is somewhat insensitive to E_i, there is first a small increase in this percent energy transfer and then a decrease as E_i is further increased from 10 to 110 eV. This effect was also seen in previous simulations of collisions of both $Cr^+(CO)_6$ and $(gly)_3H^+$ with diamond {1 1 1} [17,18]. For each E_i the $(gly)_2H^+$ and $(ala)_2H^+$ collisions have similar energy transfer distributions. Their distributions for E_f, ΔE_{surf}, and ΔE_{int} are compared in Fig. 2 for collisions with $E_i = 70$ eV.

Though the energy transfer efficiencies are similar for $(gly)_2H^+$ and $(ala)_2H^+$, there are several noteworthy differences. Energy transfer to $(ala)_2H^+$ is slightly more efficient than to $(gly)_2H^+$, which is consistent with the former peptide having two additional torsional degrees of freedom (i.e., CH_3 rotors). Previous trajectory studies [18] have shown that peptide torsional degrees of freedom are preferentially excited, when the peptide is collisionally activated. At the highest initial energies of 70 and 110 eV, collisions of $(gly)_2H^+$ transfer approximately 5% more energy to the surface than do $(ala)_2H^+$ collisions. Concomitant with this difference is an increase in energy remaining in translation for the $(ala)_2H^+$ collisions.

3.2. AMBER and AM1 intramolecular potentials

In previous work, the effect of using either the AMBER empirical model or the AM1 semiempirical electronic structure theory model for the peptide ion's intramolecular potential was investigated in a simulation of protonated glycine collisions with the diamond {1 1 1} surface [19]. Simulations with these two models for $glyH^+$ give energy transfer distributions which are statistically the same [19]. The same result is found here for $(gly)_2H^+$ collisions with the diamond {1 1 1} surface, for which the distributions of energy transfer to ΔE_{int}, ΔE_{surf}, and E_f are given in Fig. 3. The incident energy and angle are 70 eV and 45°. For AMBER the average percent transfer of E_i to ΔE_{int}, ΔE_{surf}, and E_f are 15, 25, 60, while these respective average percents are 13, 26, and 61 for the AM1 model. The previous simulations for $glyH^+$ [19] and the current ones for $(gly)_2H^+$ support the use of the AMBER intramolecualr potential model in studies of energy transfer in peptide ion SID.

It is a significant finding that the AMBER and AM1 intramolecular potentials for the peptide ions give nearly identical energy transfer efficiencies. This suggests the collisional energy transfer is direct, impulsive, occurs in a short-time and, thus, is only influenced by the peptide ion's structure [35] and the forces about the ion's potential energy

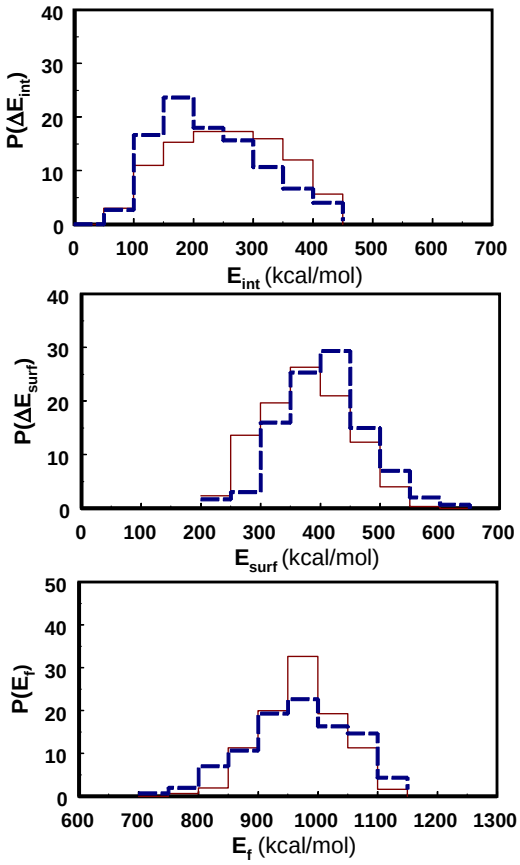

Fig. 2. Comparison of energy transfers to protonated diglycine vs. dialanine. Distributions of energy transfer to the peptide, ΔE_{int}, and to the surface, ΔE_{surf}, and of the energy remaining in translation, E_f, for $(gly)_2H^+$ (– – –) and $(ala)_2H^+$ (—) collisions with the diamond {1 1 1} surface at $E_i = 70$ eV (1614 kcal/mol) and $\theta_i = 45°$. Calculations with the AMBER potential.

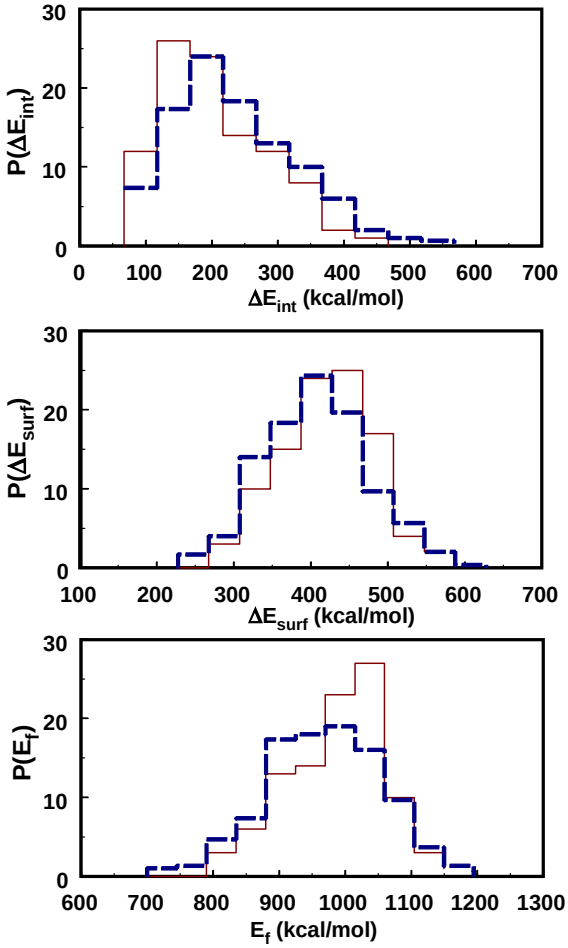

Fig. 3. Effect of peptide ion intramolecular potential on energy transfer. Distributions of energy transfer to ΔE_{int}, ΔE_{surf}, and E_f for $(gly)_2H^+$ collisions with the diamond {1 1 1} surface at $E_i = 70$ eV (1614 kcal/mol) and $\theta_i = 45$. Simulations with the AMBER (– – –) and AM1 (—) models for the $(gly)_2H^+$ intramolecular potential are compared.

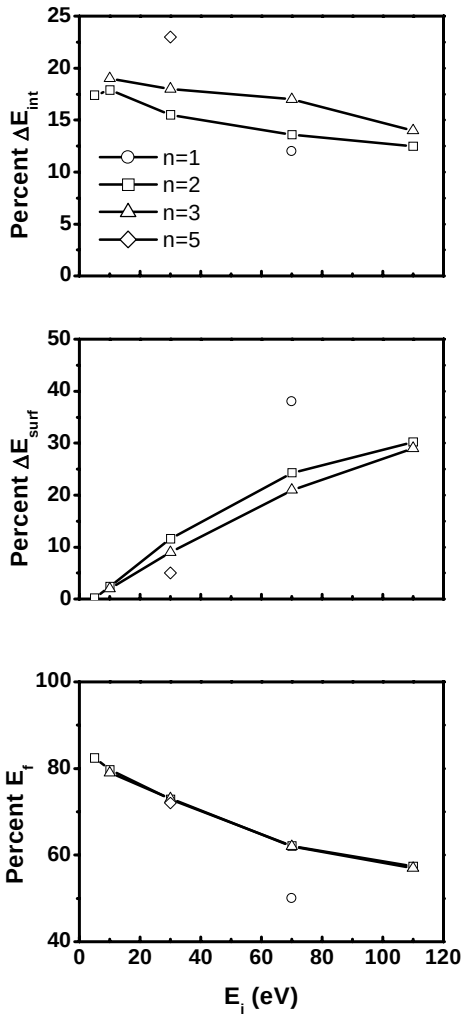

Fig. 4. Effect of peptide ion size on energy transfer. Average percent energy transfer to ΔE_{int}, ΔE_{surf}, and E_f vs. E_i for $(gly)_nH^+$ collisions with the diamond {1 1 1} surface at $\theta_i = 45^\circ$. (○) $n = 1$; (□) $n = 2$; (△) $n = 3$; and (◇) $n = 5$. Calculations with the AMBER potential and for folded peptide structures; i.e., Ref. [18]. The results reported here for $(gly)_3H^+$ at $E_i = 10$ eV are slightly different than the results in Ref. [18]. The previous results were based on a small sample size, while the current results are based on 300 trajectories for $(gly)_3H^+$.

minimum. The independence of energy transfer in SID and CID [19] on the details of the peptide ion's intramolecular potential is important and will certainly be addressed again in future studies.

3.3. Varying the peptide size

In previous simulations [18,19], energy transfer efficiencies have been determined for protonated glycine, triglycine, and pentaglycine ions colliding with the diamond {1 1 1} surface at a collision angle of 45°. As discussed before [18], energy transfer is similar for the $(gly)_3H^+$ and $(gly)_5H^+$ ions with a slightly greater average percent transfer to ΔE_{int} for the larger $(gly)_5H^+$ ion. Here, the energy transfer efficiencies determined in the previous studies are combined with those obtained from the current work to compare average percent energy transfers to ΔE_{int}, ΔE_{surf}, and E_f for the $(gly)_nH^+$ ions, $n = 1$–3, 5. The comparison is made in Fig. 4.

3.4. Varying the collision angle

Experimental studies of peptide ion SID have been performed at different collision angles; e.g., at θ_i of 0° (normal to the surface) and at 45° as for the above simulations. In the simplest models of energy transfer in gas–surface collisions [36], it is only the normal component E_i^n of E_i which participates in energy transfer. However, with surface roughness and anisotropy in the gas–surface interaction, the parallel component E_i^p may also induce energy transfer (i.e., $E_i = E_i^n + E_i^p$) [37,38]. The following investigates how varying θ_i from 45 to 0° affects energy transfer from E_i to ΔE_{int}, ΔE_{surf}, and E_f in $(gly)_2H^+$ + diamond {1 1 1} collisions.

Average percent energy transfers to ΔE_{int}, ΔE_{surf}, and E_f versus E_i are plotted in Fig. 5 and compared in Table 1

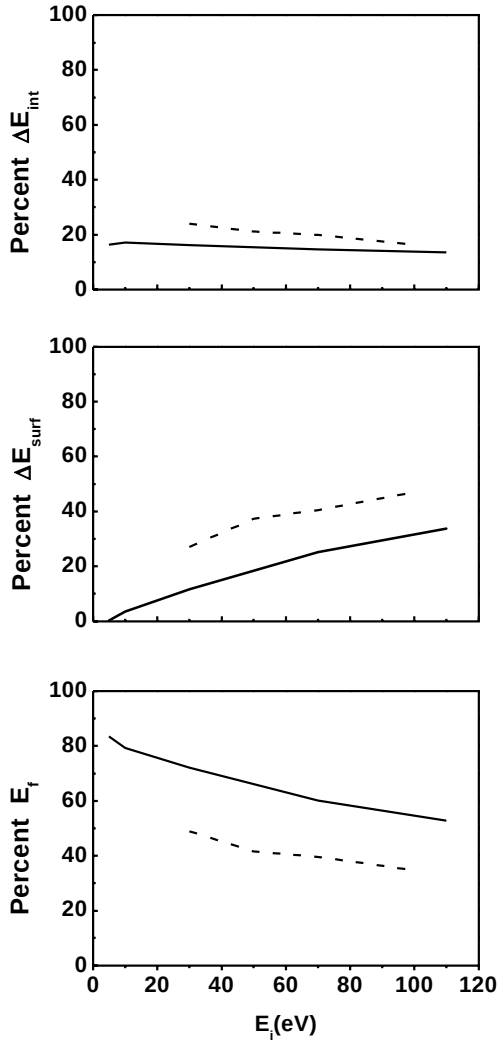

Fig. 5. Effect of collision angle on energy transfer. Average percent energy transfer to ΔE_{int}, ΔE_{surf}, and E_f vs. E_i for $(\text{gly})_2\text{H}^+$ collisions with the diamond $\{1\,1\,1\}$ surface at θ_i of 0° (– – –) and 45° (—).

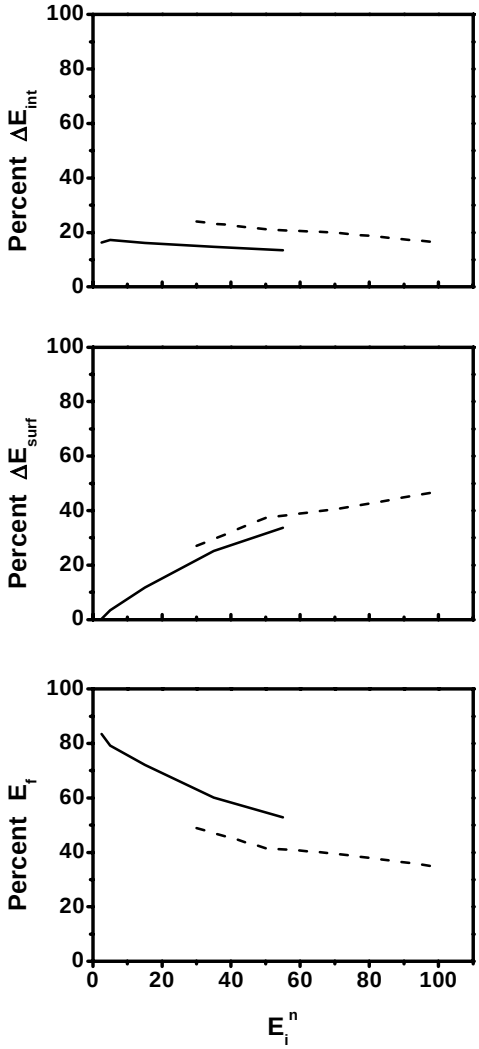

Fig. 6. Effect of collision angle on energy transfer. Average percent energy transfer to ΔE_{int}, ΔE_{surf}, and E_f vs. E_i^n, normal component of E_i, for $(\text{gly})_2\text{H}^+$ collisions with the diamond $\{1\,1\,1\}$ surface at θ_i of 0° (– – –) and 45° (—).

for $(\text{gly})_2\text{H}^+$ colliding with diamond $\{1\,1\,1\}$ at θ_i of 0 and 45°. For the calculations at $\theta_i = 45°$ AMBER is used for the $(\text{gly})_2\text{H}^+$ intramolecular potential, while AM1 is used for the $(\text{gly})_2\text{H}^+$ potential at $\theta_i = 0°$ [26]. However, as shown above, the results are insensitive to whether AMBER or AM1 is used for the $(\text{gly})_2\text{H}^+$ potential. The results in Fig. 5 show that changing θ_i from 0 to 45° decreases the energy transfer to ΔE_{int} and ΔE_{surf}, and retains more energy in E_f. Of the three energy transfers, that for ΔE_{int} is least sensitive to the collision angle. The trends found here for the dependence of energy transfer to ΔE_{int}, ΔE_{surf}, and E_f on collision angle are in qualitative agreement with experiments by Hermann and co-workers [37,38]. However, they find that energy transfer to ΔE_{int} is independent of incident angle for collisions with alkyl thiolate self-assembled monolayers (SAMs). These experimentally prepared surfaces may be rougher than the smooth diamond $\{1\,1\,1\}$ surface investigated here, which would have the effect of making energy transfer to ΔE_{int} less dependent on collision angle. The manner in which the incident angle affects energy transfer to ΔE_{int} may be different for diamond and hydrocarbon SAM surfaces. In future simulations, it will be important to determine how the incident angle affects energy transfer in collisions of protonated peptide ions with hydrocarbon SAM surfaces.

In Fig. 6 the average percent energy transfers to ΔE_{int}, ΔE_{surf}, and E_f are plotted versus the normal component of E_i, i.e., $E_i^n = E_i \cos^2 \theta_i$. As in Fig. 5, the results are for $(\text{gly})_2\text{H}^+$ colliding with diamond $\{1\,1\,1\}$ at θ_i of 0 and 45°. The energy transferred to the surface, ΔE_{surf}, scales best with E_i^n. The energy that remains in translation, E_f, scales better with E_i^n than E_i, but the relationship is still poor. Energy transfer to ΔE_{int} scales better with E_i than E_i^n. Overall, neither E_i or E_i^n gives a good representation of the energy transfers to ΔE_{int}, ΔE_{surf}, and E_f versus incident angle.

4. Questions for future studies

This study has provided important new information concerning the ways in which peptide SID is affected by: (1) the peptide's amino acids, i.e., glycine versus alanine; (2) the intramolecular potential energy function used for the peptide, i.e., AMBER versus AM1; (3) the peptide's size; and (4) the collision angle. However, the study has raised and leaves open several important issues which should be addressed in future studies. They are:

1. As the collision energy is increased, the percent energy transfer to the diamond {1 1 1} surface increases and the percent which remains in translation decreases. At the low collision energy of 5 eV, energy transfer to the surface is of the order of 1% or less. The increase in energy transfer to the surface is consistent with an effective "softening" of the surface as the translational velocity is increased [39]. However, as energy transfer to surface vibration increases as E_i is increased, there is not a corresponding increase in percent energy transfer to ΔE_{int} the peptide's vibrational degrees of freedom. Instead, the percent energy transfer to ΔE_{int} decreases as E_i is increased from 10 to 110 eV. The same type of increase in energy transfer to the surface and decrease in energy transfer to the projectile's vibrations, with increase in E_i, is seen in simulations of $(gly)_3H^+$ and $Cr(CO)_6{}^+$ collisions with diamond {1 1 1} [18,19].
2. For $Cr(CO)_6{}^+$ collisions with the *n*-hexylthiolate SAM surface, percent energy transfer to ΔE_{int} is nearly constant and independent of E_i, while percent energy transfer to ΔE_{surf} first increases and then approaches on apparent limiting values of ~80% at high E_i [40]. This asymptotic value is the same as that for Ne atom collisions with this SAM [41]. It would be of interest to determine whether peptide ions have the same trends in efficiencies of energy transfer versus E_i when colliding with the SAM. Also of interest would be to determine whether the diamond {1 1 1} surface has a high E_i asymptotic limiting value for average percent energy transfer to ΔE_{surf} as for the SAM surface.

Acknowledgements

This research was supported by the National Science Foundation. The authors wish to thank Tianying Yan and Lipeng Sun for their assistance and very helpful discussions.

References

[1] B.E. Winger, H.-J. Laue, S.R. Horning, R.K. Julian Jr., S.A. Lammert, D.E. Riederer Jr., R.G. Cooks, Rev. Sci. Instrum. 63 (1992) 5613.
[2] A.L. McCormack, A. Somogyi, A. Dongré, V.H. Wysocki, Anal. Chem. 65 (1993) 2859.
[3] J.A. Burroughs, S.B. Wainhaus, L. Hanley, J. Phys. Chem. 98 (1994) 10913.
[4] R. Wörgötter, V. Grill, Z. Herman, H. Schwarz, T.D. Märk, Chem. Phys. Lett. 270 (1997) 333.
[5] R.G. Cooks, T. Ast, T. Pradeep, V. Wysocki, Acc. Chem. Res. 27 (1994) 316.
[6] J.L. Jones, A.R. Dongré, A. Somogyi, V.H. Wysocki, J. Am. Chem. Soc. 116 (1994) 8368.
[7] M. Meot-Ner (Mautner), A. Dongré, A. Somogyi, V.H. Wysocki, Rapid Commum. Mass Spectrom. 9 (1995) 829.
[8] A.R. Dongre, J.L. Jones, A. Somogyi, V.H. Wysocki, J. Am. Chem. Soc. 118 (1996) 8365.
[9] G. Tsaprailis, H. Nair, A. Somogyi, V.H. Wysocki, W. Zhong, J.H. Futrell, S.G. Summerfield, S.J. Gaskell, J. Am. Chem. Soc. 121 (1999) 5142.
[10] H. Lim, D.G. Schultz, C. Yu, L. Honley, Anal. Chem. 71 (1999) 2307.
[11] D.G. Schultz, H. Lim, S. Garbis, L. Hanley, J. Mass. Spectrom. 34 (1999) 217.
[12] J. Laskin, E. Denisov, J.H. Futrell, J. Am. Chem. Soc. 122 (2000) 9703.
[13] J. Laskin, E. Denisov, J.H. Futrell, J. Am. Phys. Chem. B 105 (2001) 1895.
[14] J. Laskin, J.H. Futrell, J. Chem. Phys. 116 (2002) 4302.
[15] D.G. Schultz, S.B. Wainhaus, L. Hanley, P. de Sainte Claire, W.L. Hase, J. Chem. Phys. 106 (1997) 10337.
[16] S.B.M. Bosio, W.L. Hase, Int. J. Mass Spectrom. Ion Processes 174 (1998) 1.
[17] O. Meroueh, W.L. Hase, Phys. Chem. Chem. Phys. 3 (2001) 2306.
[18] O. Meroueh, W.L. Hase, J. Am. Chem. Soc. 124 (2002) 1524.
[19] O. Meroueh, Y. Wang, W.L. Hase, J. Phys. Chem. A 106 (2002) 9983.
[20] M.R. Morris, D.E. Riederer Jr., B.E. Winger, R.G. Cooks, T. Ast, C.E.D. Chidsey, Int. J. Mass Spectrom. Ion Processes 122 (1992) 181.
[21] W.D. Cornell, P. Cieplak, C.I. Bayley, I.R. Gould, K.M. Merz, D.M. Ferguson, D.C. Spellmeyer, T. Fox, J.W. Caldwell, P.A. Kollman, J. Am. Chem. Soc. 117 (1995) 5179.
[22] M.J.S. Dewar, E.G Zoebisch, E.F. Healy, J.J.P. Stewart, J. Am. Chem. Soc. 107 (1985) 3902.
[23] W.L. Hase, R.J. Duchovic, X. Hu, A. Komornicki, K.F. Lim, D.-h Lu, G.H. Peslherbe, K.N. Swamy, S.R. Vande Linde, L. Zhu, A. Varandas, H. Wang, R.J. Wolf, QCPE 16 (1996) 671.
[24] J.J.D. Stewart, MOPAC 7.0, A public domain general molecular orbital package (QCPE 457 7.0), Quantum Chemistry Program Exchange, No. 455, 13, (1993) 42–45.
[25] G.H. Peslherbe, C. Doubleday Jr., W.L. Hase, in preparation.
[26] Y. Wang, W.L. Hase, unpublished results.
[27] K.C. Hass, M.A. Tamor, T.R. Anthony, W.F. Banholzer, Phys. Rev. B 45 (1992) 7171.
[28] D.L. Bunker, Methods Comput. Phys. 10 (1971) 287.
[29] D.L. Bunker, Acc. Chem. Res. 7 (1974) 195.
[30] S. Chapman, D.L. Bunker, J. Chem. Phys. 62 (1975) 2890.
[31] C.S. Sloane, W.L. Hase, J. Chem. Phys. 66 (1977) 1523.
[32] Y.J. Cho, S.R. Vande Linde, L. Zhu, W.L. Hase, J. Chem. Phys. 85 (1992) 958.
[33] G.H. Peslherbe, H. Wang, W.L. Hase, in: D. Ferguson, J.I. Siepmann, D.G. Truhlar (Eds.), Advances in Chemical Physics, vol. 105, Wiley, New York, 1999, p. 171.
[34] M.P. Allen, D.J. Tildesley, Computer Simulation of Liquids, Oxford University Press Inc., New York, 1987.
[35] O. Meroueh, W.L. Hase, J. Phys. Chem. A 103 (1999) 3981.
[36] F.O. Goodman, H.Y. Wachman, Dynamics of Gas–Surface Scattering, Academic Press, New York, 1976.

[37] J. Kubišta, Z. Dolejšek, Z. Hermann, Eur. Mass Spectrom. 4 (1998) 311.
[38] J. Žabka, Z. Dolejšek, Z. Hermann, J. Phys. Chem A 106 (2002) 10861.
[39] H.K. Shin, in: W.H. Miller (Ed.), Dynamics of Molecular Collision, Part A, Plenum, New York, 1976, p. 131.
[40] K. Song, O. Meroueh, W.L. Hase, J. Chem. Phys. 118 (2003) 2893.
[41] S.B.M. Bosio, W.L. Hase, J. Chem. Phys. 107 (1997) 9677.